JOURNAL OF MATERIALS SCIENCE 32 (1997) 3807–3812

Processing of spodumene-modified mullite ceramics

I. M. LOW*, E. MATHEWS, T. GARROD, D. ZHOU
Materials Research Group, School of Physical Sciences, Curtin University of Technology, GPO Box U1987, Perth, WA 6001, Australia

D. N. PHILLIPS, X. M. PILLAI
School of Applied Chemistry, Curtin University of Technology, GPO Box U1987, Perth, WA 6001, Australia

The use of β-spodumene ($Li_2O \cdot Al_2O_3 \cdot 4SiO_2$) has been investigated as a liquid-phase sintering aid for the densification of mullite processed from fumed silica and ESP (alumina) dust. XRD, DTA, SEM and Vickers indentation were used to characterize the effect of spodumene on the phase relations, sintering behaviour, microstructure and mechanical properties of mullite. The results show that the presence of spodumene significantly reduces the porosity, improves the sintering behaviour and enhances the formation of mullite at 1550 °C. Spodumene-modified mullite ceramics also have better physical and mechanical properties.

1. Introduction

Mullite is an important class of engineering ceramics which possesses excellent thermal and mechanical properties. In particular, its low thermal expansion coefficient makes the material very resistant to thermal shock. Numerous methods have been used to synthesize stoichiometric mullite with the composition $3Al_2O_3 \cdot 2SiO_2$. These include clays [1] and precursors of Al_2O_3 and SiO_2 [2–9]. Recently Hong *et al.* [10] and Mizuno and Saito [11] have synthesized low cost high-purity mullite powders from silica fume–aluminium nitrate and silica fume–aluminium salts, respectively. Using fumed silica and alumina, high yield but porous mullite-based ceramics have been fabricated by Grace *et al.* [12,13]. The high porosity was attributed to the agglomeration of fumed particles during sintering. This suggests that the use of a flux as a liquid phase sintering aid is vital for reducing the porosity in these materials. One such flux is spodumene ($Li_2O \cdot Al_2O_3 \cdot 4SiO_2$).

Spodumene has been widely used in the glass and ceramic industry for decades as a lithia-bearing flux and low-expansion filler in whiteware bodies [14]. It is used for making glasses and ceramics harder, smoother, chemical and thermal shock resistant [15,16]. Recently, Latella *et al.* [17] have utilized spodumene as a liquid-phase sintering aid for the densification of alumina ceramics (99.8% dense) at 1500 °C.

The α-polymorph of spodumene is a monoclinic pyroxene which is stable under ambient conditions. This phase undergoes an irreversible phase change at 1080 °C, forming the more open tetragonal polymorph, β-spodumene, which melts at 1423 °C. The transformation is accompanied by a 30% volume increase due to a density change from 3.2 to 2.4 $g\,cm^{-3}$ [16].

This paper describes the use of spodumene as a flux and a filler for cost-effective processing of mullite ceramics. The effect of spodumene on the sintering behaviour, phase relation and properties is discussed.

2. Experimental procedure

2.1. Powder processing

Commercial silica fume (supplied by Simcoa Operations), electrostatic precipitated (ESP) alumina dust (supplied by Alcoa of Australia), and β-spodumene powder concentrate (supplied by Gwalia Consolidated Ltd) were used as the starting materials for the synthesis of mullite ceramics. Silica fume contained 4.6 wt % residual carbon and approximately 1.5 wt % SiC. The spodumene powder was a calcined concentrate and had a mean particle size of 23 μm. A mixture of gibbsite (≈24 wt %) and α-Al_2O_3 was present in the ESP dust [18]. The chemical analyses of these starting raw materials are shown in Table I. Conventional ceramic processing routes were used to prepare spodumene-modified (3 : 2) mullite ceramics containing 5–30 wt % spodumene. Table II lists the formulations for each of the samples. Each batch was mixed by attrition milling in a Teflon jar filled with

* Author to whom all correspondence should be addressed.

0022–2461

TABLE I Chemical analyses (wt %) of starting raw materials

	Spodumene	Silica fume	ESP dust
Al_2O_3	27.0	0.13	89.4
SiO_2	64.0	88.9	0.28
C	–	4.6	–
SiC	–	1.5	–
S	–	–	0.09
Li_2O	8.10	–	–
Fe_2O_3	0.16	0.07	0.12
CaO	0.04	0.08	0.39
MgO	0.02	0.5	0.02
Na_2O	0.19	–	1.03
K_2O	0.05	0.24	<0.01
TiO_2	0.02	0.01	0.01
P_2O_5	0.11	–	0.02
LOI	0.46	4.0	8.80

TABLE II Formulations of various mullite ceramics

Sample	Silica fume (wt %)	ESP dust (wt %)	Spodumene
SPM0	28	72	0
SPM5	28	72	5
SPM10	28	72	10
SPM20	28	72	20
SPM30	28	72	30

deionized water and alumina–silica media for 2 h. Three wt % of polyethylene glycol (PEG) was added as a binder to each batch after 1.5 h milling and thoroughly mixed for a further 0.5 h, after which the contents were sieved through a 45 mm sieve and oven dried for 24 h at 105 °C. The dessicated mass was then granulated with a mortar and pestle to pass through a 710 μm sieve.

Disc samples of 15 mm diameter and 4 mm thickness were fabricated by uniaxial pressing at 150 MPa using a mild-steel die assembly. The green disc samples were placed on high-purity alumina plates packed with loose bedding alumina for firing. The heat-treatment cycle involved a heating rate of 5 °C min^{-1} to 600 °C with a dwell time of 1 h, followed by heating at 10 °C min^{-1} to 1300 °C with 2 h dwelling time, before the final sintering step at 1550 °C for 3 h. Samples were cooled to room temperature at a rate of 8 °C min^{-1}. All firings were performed in a Thermolyne high temperature furnace.

2.2. Materials characterization

Particle size distributions of silica fume and ESP dust were measured on a Malvern Master Sizer. The particle size distribution of the ESP dust showed a mean particle size of 8 μm (Fig. 1) and a specific surface area of 1.58 $m^2 g^{-1}$ [18]. Particle size distributions of unfired silica fume (Fig. 2) shows the typical bimodal particle size distribution where approximately 50% of the particles were below 1 μm. Fig. 3 shows the tendency of fume particles to agglomerate with an attendant change to a unimodal distribution with a 7 μm peak when the fume was fired at 600 °C for 0.5 h [12,13]. DTA measurements on the powder mixture were carried out on a Stanton Redcroft STA-780 to monitor the formation of mullite. There was no evidence of mullite exotherms at 970 and 1250 °C (Fig. 4) because of the sluggish reaction between silica fume and ESP dust under those conditions [12,13].

Analysis of phases formed and their abundance was performed with a Siemens D500 X-ray diffractometer.

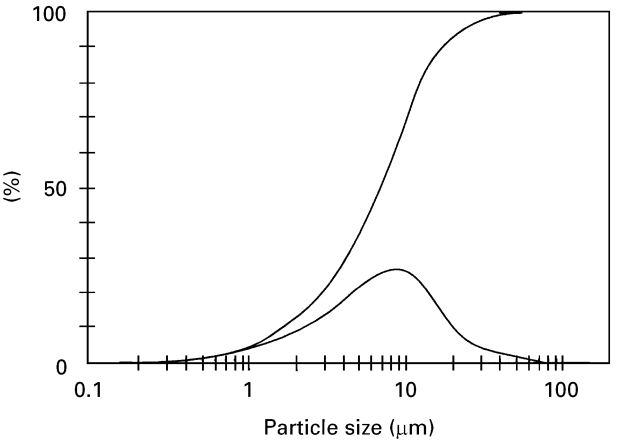

Figure 1 Particle size distribution of ESP dust.

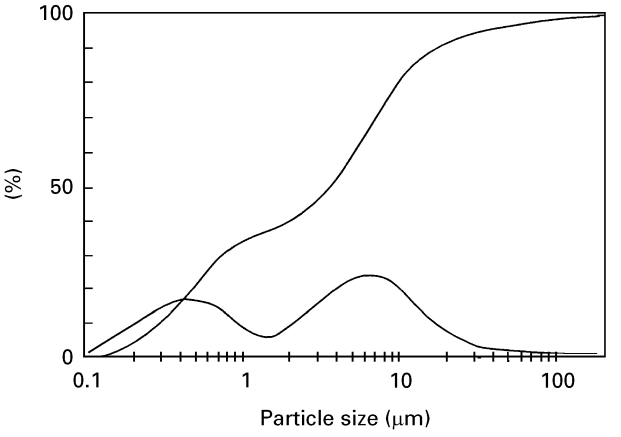

Figure 2 Bimodal particle size distribution of as-received silica fume.

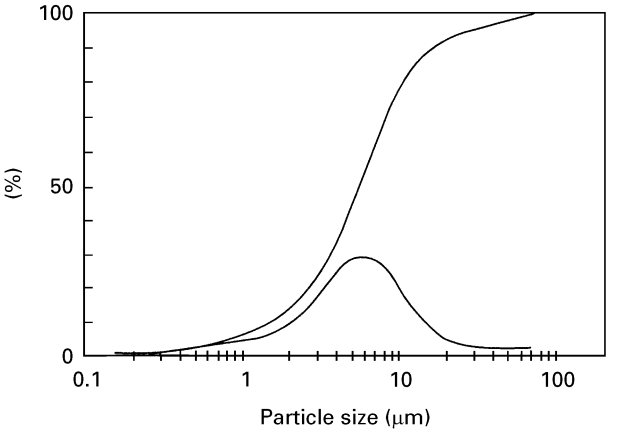

Figure 3 Unimodal distribution of silica fume heat-treated at 600 °C for 0.5 h.

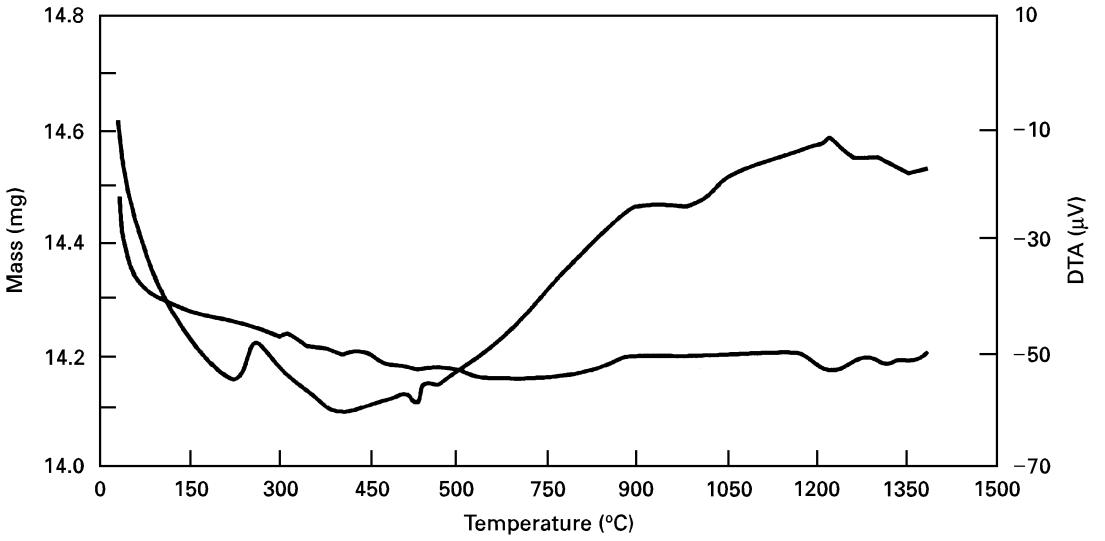

Figure 4 Thermogram of sample SPM0.

The operating conditions used were: CuK_α radiation ($l = 0.15418$ nm) produced at 40 kV and 30 mA, 1° divergence for the incident beam and 0.15° receiving slit, goniometer range = 10–130°, step size = 0.04, counting time 1 s/step, and post-diffraction graphite monochromator with NaI detector and PHA.

The relative concentrations (C) of mullite (m) and alumina (a) present in the microstructure was computed using the following equation:

$$C_m/C_a = (K_m/K_a)\,[(l/l_c)_m/(l/l_c)_a] \quad (1)$$

where K_m/K_a is the scaling factor of mullite to alumina, and $(l/l_c)_m/(l/l_c)_a$ is a ratio of corundum (c) scaling factors of mullite to alumina.

The Australian Standard AS 1774.5 [19] was used to evaluate bulk density and apparent porosity. Both microhardness and fracture toughness (K_{IC}) of polished samples were measured using a Tukon microhardness tester at a maximum load of 1.0 kg. The lengths of both diagonals of the impression and the radial cracks (c) were measured and K_{IC} determined using the method suggested by Anstis *et al.* [20], i.e.

$$K_{IC} = 0.16(E/H)^{1/2}(P/c)^{3/2} \quad (2)$$

where H is the hardness and E is the elastic modulus.

3. Results and discussion

3.1. Phase relations

Mullite is the only compound formed in the alumino–silicate system. There exists two forms of mullite, namely (2:1) and (3:2) mullite with compositions of $2Al_2O_3 \cdot SiO_2$ and $3Al_2O_3 \cdot 2SiO_2$, respectively. Table III shows the phases formed and their abundance in various samples. Mullite is clearly seen in all the samples together with unreacted corundum. Neither cristobalite nor other phases could be detected. These results agree fairly well with theoretical reactions between Al_2O_3 and SiO_2 to form mullite which may be summarized as follows [7]:

TABLE III Phase abundance of various mullite ceramics

Sample	Mullite (wt %)	α-Al_2O_3 (vol %)	Cristobalite
SPM0	86	14	–
SPM5	92	8	–
SPM10	95	5	–
SPM15	95	5	–
SPM20	96	4	–
SPM30	94	6	–

$$3Al_2O_3 + 2SiO_2 \rightarrow 3(Al_4 \cdot SiO_8) + SiO_2 \quad (3)$$

$$3(Al_4 \cdot SiO_8) \rightarrow 3(Al_2O_3 \cdot SiO_2) \quad (4)$$

$$3(2Al_2O_3 \cdot SiO_2) + SiO_2 \rightarrow 2(3Al_2O_3 \cdot 2SiO_2) \quad (5)$$

Reaction 3 is exothermic and is believed to take place at approximately 970 °C forming Al–Si spinel and amorphous SiO_2. As mentioned previously, the absence of an expected exotherm in the DTA plot could be attributed to the difficulty of achieving complete homogeneity between silica fume and ESP dust, thus leading to a very sluggish and diluted reaction. As the temperature increases, the spinel transforms to an alumina-rich (2:1) mullite as depicted by Reaction 4. The aluminous mullite then reacts with silica to form the equilibrium (3:2) mullite at approximately 1250 °C. This suggests that mullite is a solid-solution at a range of 72–80 wt % Al_2O_3. Hence all the samples should have fully converted to yield 100% mullite. The slightly lower yields obtained in these samples may be attributed to the difficulty of mixing Al_2O_3 and SiO_2 to achieve 100% homogeneity which is essential for complete reaction. Clearly an improved mixing and attrition method is required to achieve full mullitization in these samples. In spite of this, the results clearly indicate that silica fume and ESP dust can be used as a cheap raw material for synthesizing

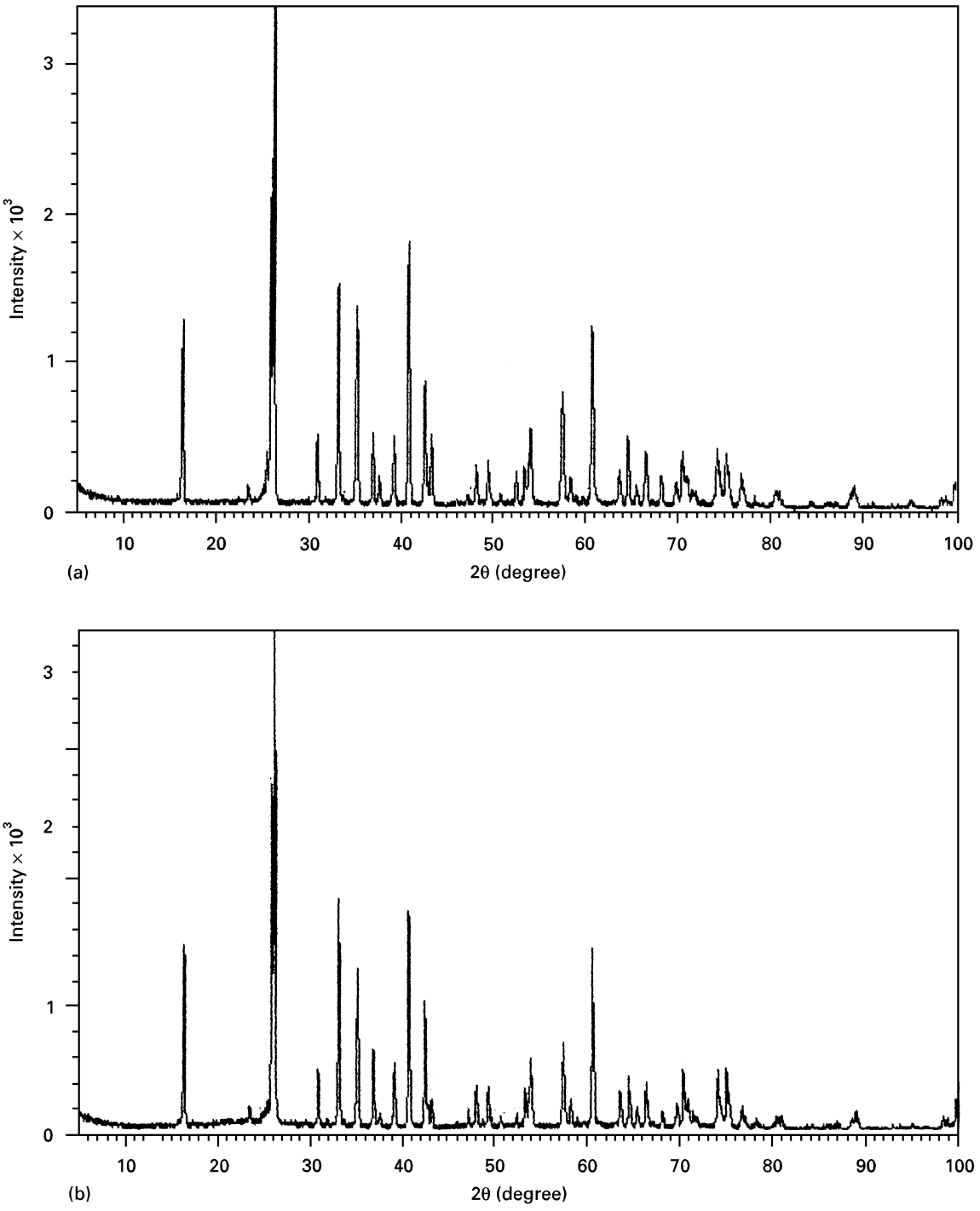

Figure 5 X-ray diffraction patterns of (a) pure mullite and (b) spodumene-modified mullite (SPM15).

fine grained mullite ceramics [12]. It is interesting to note that the presence of spodumene improved the sintering behaviour of mullite. Similar improvement in sintering was observed by Latella *et al.* [17] in their processing of alumina ceramics. Also the presence of 20 wt % spodumene enhanced the formation of mullite and raised its yield from 86% to a maximum of 96% (see Table III). It is postulated that the dissociated silica from the phase separation of spodumene at high temperatures reacted with any excess alumina to form mullite. The X-ray diffraction patterns for both pure and spodumene-modified mullite are depicted in Fig. 5.

3.2. Physical and mechanical properties

Table IV shows the density, porosity, hardness and fracture toughness of sintered mullite samples. Poor densification of pure mullite is evident from its high porosity. This can be attributed to the presence of ESP dust (~ 8 μm) and fumed silica (~ 7 μm) with a relatively coarse mean particle size, and their tendency to agglomerate during calcination. Use of attrition or milling to reduce the particle size of these powders should improve the densification and reduce the porosity significantly. Similar problems with densification were observed by Dean *et al.* [18] in their attempt to use ESP dust for fabricating alumina-based ceramics,

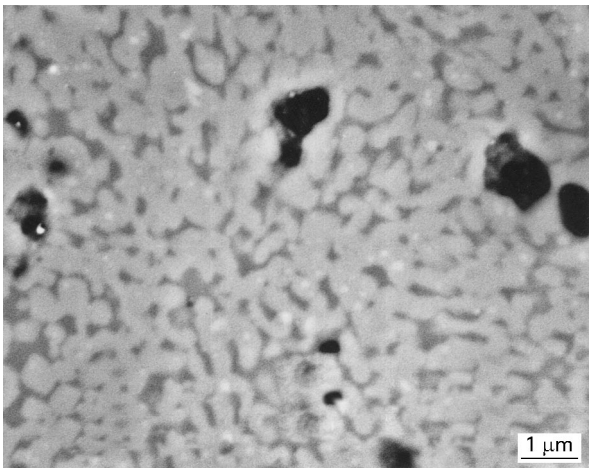

Figure 6 Back-scattered electron micrograph showing the fine-grained microstructure of mullite sample (SPM10).

TABLE IV Physical and mechanical properties of various spodume-modified mullite ceramics

Sample	Density ($g\ cm^{-3}$)	Porosity (%)	Hardness (GPa)	K_{IC} ($MPa\ m^{1/2}$)
SPM0	2.09	33	6	2.8–3.0
SPM5	2.51	16	11	2.8–3.2
SPM10	2.54	14	6	2.4–3.5
SPM15	2.48	9	9	2.4–3.1
SPM20	2.38	7	7	2.5–3.2
SPM30	2.28	13	5	2.7–3.3

where porosities in the range 18–51% were obtained. It is believed that the prevalence of intra-agglomerate sintering and no inter-agglomerate sintering are the causes for the formation of the large number of pores. Similar observations have been made by Hong *et al.* [10] in their attempt to densify mullite powders derived from silica fume and aluminium nitrate. The presence of spodumene significantly reduced the porosity from 33 to 7% via the formation of a liquid phase at 1423 °C. This liquid phase serves not only to reduce de-agglomeration but also intra-agglomeration during sintering. The fine-grained microstructure of spodumene-modified mullite is shown in Fig. 6. The gain structure is equiaxed and of narrow size distribution. The pores formed predominantly at triple joint junctions. The mean size for the mullite grains is approximately 1.50 μm.

The hardness value of 5 wt % spodumene-modified mullite is considerably higher than that of pure mullite (Table IV). The improvement in hardness is in accordance with a denser microstructure. Addition of more spodumene did not appear to raise the hardness in spite of much reduced porosity. Similar reduction in hardness was obtained for alumina ceramics as the content of spodumene increased [17]. This may be explained by the presence of relatively soft spodumene which serves to counterbalance any improvement in porosity reduction. It is difficult to evaluate the effect of spodumene on fracture toughness, K_{IC}, due to a large scatter of results. It appears that K_{IC} of mullite was basically unaffected by the presence of spodumene. The presence of spodumene was also observed not to influence the K_{Ic} of alumina ceramics [17]. Although not measured, the presence of spodumene is expected to improve the modulus of rupture and thermal shock resistance of mullite by virtue of better densification and lower coefficient of thermal expansion. The work on evaluation of thermal shock performance of spodumene-modified mullite ceramics is in progress and the results will be reported in due course.

4. Conclusion

High yield spodumene-modified mullite-based ceramics have been readily produced by the reaction between relatively low-cost silica fume and ESP alumina dust, with spodumene acting as flux and filler. The presence of spodumene provided an effective sintering flux to enhance the degree of mullitization and hence the yield of mullite. It also imparted better physical and mechanical properties to the mullite.

Acknowledgements

The authors thank Simcoa Operations and Alcoa (Australia) for supplying silica fume and ESP dust, respectively. We are grateful to our colleagues Professor D.-Y. Li and Ms B.-K. Gan for advice on quantitative analysis of XRD data. IML is grateful to AINSE for funding and to S. Leung of Ansto for helping with scanning electron microscopy.

References

1. G. W. BRIDLEY and M. NAKAHIRA, *J. Amer. Ceram. Soc.* **42** (1959) 311.
2. L. B. PANKRATZ, W. W. WELLER and K. K. KELLEY, *US Bur. Mines, Rep. Invest.* **6287** (1963) 6.
3. R. ROY, *J. Amer. Ceram. Soc.* **39** (1956) 145.
4. Y. HIRATA, K. SAKEDA, Y. MATSUSHITA and K. SHIMADA, *Yogyo Kyokaishi* **93** (1983) 874.
5. D. W. HOFFMAN, R. ROY and S. KOMARNENI, *J. Amer. Ceram. Soc.* **67** (1984) 468.
6. M. G. ISMAIL, Z. NAKAI and S. SOMIYA, *ibid.* **70** (1987) C-7.
7. I. M. LOW and R. McPHERSON, *J. Mater. Sci.* **24** (1989) 926.
8. J. D. CROFTS and W. W. MARSHALL, *Trans. Brit. Ceram. Soc.* **66** (1967) 121.
9. S. OTANI and A. KOJIMA, *Kogyo Kagaku Zasshi* **67** (1964) 1509.
10. C. S. HONG, P. RAVINDRANATHAN, D. K. AGRAWAL and R. ROY, *J. Mater. Sci. Lett.* **13** (1994) 1072.
11. M. MIZUNO and H. SAITO, *J. Amer. Ceram. Soc.* **72** (1989) 377.
12. A. GRACE, I. M. LOW, K. ABDULLAH, G. BURTON, D. ZHOU, R. SKALA, D. PHILLIPS and Z. PILLAI, *J. Mater. Sci. Lett.* **14** (1995) 1310.
13. A. GRACE, I. M. LOW, R. SKALA, D. PHILLIPS and Z. PILLAI, in Proceedings of the International Ceramics Conference edited by C. C. Sorrell (Austceram 94), 25–27 July 1994, Sydney (Australasian Ceramic Society, Sydney, 1994) p. 886.
14. C. A. COWAN, G. A. BOLE and R. L. STONE, *J. Amer. Ceram. Soc.* **33** (1950) 193.
15. J. KUSNIK and K. W. TERRY, *Mater. Sci. Forum* **34–36** (1988) 931.
16. J. H. FISHWICK, "Applications of Lithium in Ceramics" (Cahners Books, Boston, Mass., 1974).

17. B. L. LATELLA, G. R. BUTTON and B. H. O'CONNOR, *J. Amer. Ceram. Soc.* **78** (1995) 1895.
18. G. A. DEAN, C. M. CARDILE and R. J. STEAD, Proceedings of the International Ceramics Conference (Austceram 94), Sydney, 1994, p. 1315.
19. Australian Standard AS 1774.5, "Method 5: The Determination of Density, Porosity and Water Absorption" (Australian Standards Bureau, Sydney, 1989).
20. G. R. ANSTIS, P. CHANTIKUL, B. R. LAWN and D. B. MARSHALL, *J. Amer. Ceram. Soc.* **64** (1981) 533.

Received 19 October 1995
and accepted 10 February 1997